Galvanic Corrosion Following Local Breakdown of a Scale Formed on X-65 in CO_2 Saturated Solutions

Fernández-Domene, Ramón Manuel
Universitat Politécnica de Valencia
Campus Camino de Vera s/n
Valencia, Valencia, 46022
Spain

Leiva-García, Rafael
University of Manchester
Sackville Street
Manchester, Greater Manchester, M139PL
United Kingdom

Andrews, Jake
University of Manchester
Sackville Street
Manchester, Greater Manchester, M139PL
United Kingdom

Akid, Robert
University of Manchester
Sackville Street
Manchester, Greater Manchester, M139PL
United Kingdom

ABSTRACT

Under some conditions in sweet environments, the precipitation of corrosion products (primarily $FeCO_3$) on the surface of X-65 pipeline steel can decrease the corrosion rate of the metal, this precipitated film acting like a protective scale. However, when these scales are damaged due to effects such as solid-particle erosion or mechanical stress, a galvanic pair can form between the bare steel (anode) and the surrounding undamaged scale (cathode). The aim of this work is to evaluate the magnitude of galvanic coupling that arises when the protective scale is broken and a corrosion cell is established between the defect and the surrounding scale. This study has been conducted in two stages: firstly, the formation of a protective scale on the surface of X-65 samples in CO_2 saturated conditions (80 ºC and a CO_2 pressure of 0.53 bars); secondly, a scaled sample of X-65 steel was coupled with a fresh (non-scaled) X-65 sample in a brine solution saturated with CO_2 at 60ºC. Zero resistance ammeter (ZRA) measurements were then conducted using this galvanic couple. According to the results, there was galvanic coupling between the bare metal and a scaled surface where the magnitude of the galvanic pair was found to be dependent on the anode:cathode ratio.

Key words: Galvanic pair; Sweet corrosion; ZRA; Carbon steel; X-65.

INTRODUCTION

X-65 pipeline steel in sweet environments corrodes as a consequence of the presence of CO_2; this corrosion can be favoured by the presence of chlorides or reduced by using inhibitors. However, in some cases the corrosion process can lead to the formation of protective scales resulting from the

precipitation of corrosion products. When these films are formed, they can slow the corrosion process by being a barrier to the diffusion or covering active sites. Siderite ($FeCO_3$) is the most important film, in terms of corrosion mitigation in sweet environments, the growth of this film being extremely dependent on the kinetics of precipitation. Different parameters such as, microstructure, temperature, CO_2 partial pressure and compound supersaturation, play an important role in the formation of these scales. According to literature, the presence of cementite can act like anchoring of the scales.[1] Regarding the temperature, the raise of this parameter acts in two ways; increasing the rate of the electrochemical reactions and decreasing the solubility of the iron carbonate ($FeCO_3$). On the other hand, the partial pressure of CO_2 affects the cathodic reactions and the pH of the medium. Finally, supersaturation has a fundamental role in the formation of scales, so it is important to know the concentration of compounds which lead to the formation of insoluble salts; a high supersaturation is necessary to form a protective film [2]. The layers formed as a consequence of the Fe^{2+} supersaturation can reduce the corrosion rate in different ways [3]: establishment of a diffusion layer, formation of a low porosity protective layer, reduction of the area to be corroded, or creation of concentration gradients of the main chemical species involved in the formation of scales. However, localised corrosion can take place when the protective scale is damaged locally, and may result in problems which lead to the failure of the carbon steel pipelines. Scale breakdown can occur for a variety of reasons; flow effect, mechanical breakdown, erosion or chemical dissolution.[4-8] Some authors have hypothesized that following scale damage, a galvanic effect is established between the scale covered surface (cathode) and the scale free surface (anode) leading to propagation of localized attack.[9-11]

Therefore, the aim of this work is to evaluate the magnitude of galvanic coupling that arises when the protective scale is broken and a galvanic corrosion cell is established between the defect and the surrounding scale covered surface. This study is divided in two stages; the formation of a stable scale on the surface of the X-65 and the galvanic coupling of this scaled sample with a fresh sample with different area ratios.

EXPERIMENTAL PROCEDURE

Materials

The material used in this study was API[(1)] 5L-X65 carbon steel. The maximum and minimum chemical composition of the carbon steel is shown in Table 1. The specimens were machined as square samples. Cu-Sn wires were spot welded to the samples and then mounted in resin, such that only an area of 2 cm^2 was exposed to the solution (Figure 1). The surface of the samples was polished using silicon carbide paper, progressively up to 4000 grit, prior to the electrochemical tests.

Figure 1: Samples used in the electrochemical tests.

Table 1: Chemical composition of X65 (wt. %).

	C	Si	Mn	P	S	Cr	Mo	Ni	Nb	V	Ti	Al	Cu
Max.	0.15	0.35	1.40	0.02	0.01	0.30	0.20	0.45	0.04	0.08	0.02	0.05	0.20
Min.	0.06	0.20	0.90	-	-	-	0.06	-	-	0.03	-	0.02	-

Electrochemical Tests

Electrochemical tests were conducted in two stages: first, monitoring, via electrochemical impedance spectroscopy (EIS), of the scale formation on one sample of X-65, secondly, the galvanic coupling of the scaled sample with an X-65 sample with fresh surface. All the tests were repeated in order to check the reproducibility and obtain mean values.

Stage One: Scale Formation

The electrochemical techniques used to monitor this stage were EIS and linear polarization resistance (LPR), with the open circuit potential (OCP) being recorded throughout the process. Experiments were performed in a three electrode cell with additional inlets for the condenser and the gas bubbler. An X65 sample was used as the working electrode, platinum as the counter electrode and the reference electrode was a saturated calomel electrode. The cell was placed in a water bath and heated to 80 °C. The composition of the electrolyte was 0.1 M NaCl and 1mM $FeCl_2$. Before immersing the X65 into the electrolyte, the solution was saturated with CO_2 (partial pressure of 0.53 bar). Purging with the gas was continued throughout the test to maintain a CO_2 atmosphere over the liquid surface. The pH was adjusted to 6.8 by adding NaOH 0.1 M. The oxygen level measured during the entire test was always below 240 ppb .

EIS measurements were conducted over the frequency range from 10 kHz to 10 mHz, with an AC signal amplitude of 10 mV vs OCP; LPR measurements were performed in the range of ±0.02 V vs OCP, with a scan rate of 0.125 mV/s. The tests were carried out for approximately 4-5 days, after which a reproducible protective scale had formed on the sample. The surface of the protective scale was analysed using X-ray diffraction (XRD). XRD scans, with a grazing incidence angle of 3 degrees, were performed on the sample measuring between 5 and 85 degrees. Additionally, the morphology of the scale was analysed by confocal microscopy.

Stage Two: Galvanic Coupling

A new, fresh bare X65 sample was partially coated in 45 stopping-off lacquer[†] to create a specific area ratio of protective scale: fresh surface. The selected area ratios ($A_R = A_{scaled}/A_{bare}$) were A_R = 50, A_R = 100 and A_R = 200. The scaled sample and the sample with the bare surface were connected to the VersaStat[†] potentiostat, which was used as a ZRA. The galvanic current density and galvanic potential between the pairs were measured every 0.5 s for 24 hours. The reference electrode was a Saturated Calomel Electrode (SCE). The tests were designed with the non-scaled sample as working electrode 1 and the scaled sample as working electrode 2. The electrochemical cell was placed in a water bath at 60 °C. Before immersing the electrodes, the solution was saturated with CO_2 and during the test, a CO_2 atmosphere was maintained over the liquid surface; the pH of the solution during the test was 5.5. The composition of the brine solution used during these tests is presented in Table 2. Additionally to

---

[†] Trade name

these tests, the corrosion rate of an uncoupled sample was tested in the same conditions during 24 hours to monitor the corrosion process without galvanic coupling.

Table 2: Chemical composition of typical 'Forties' field brine solution.

	NaCl	KCl	$CaCl_2$	$MgCl_2$	$SrCl_2$	$NaHCO_3$	CH_3OONa
g/l	84.40	0.37	7.64	1.09	0.42	0.64	2.38

RESULTS

Scale Formation

Figure 2 presents Nyquist diagrams of the X65 sample after different scale formation times.
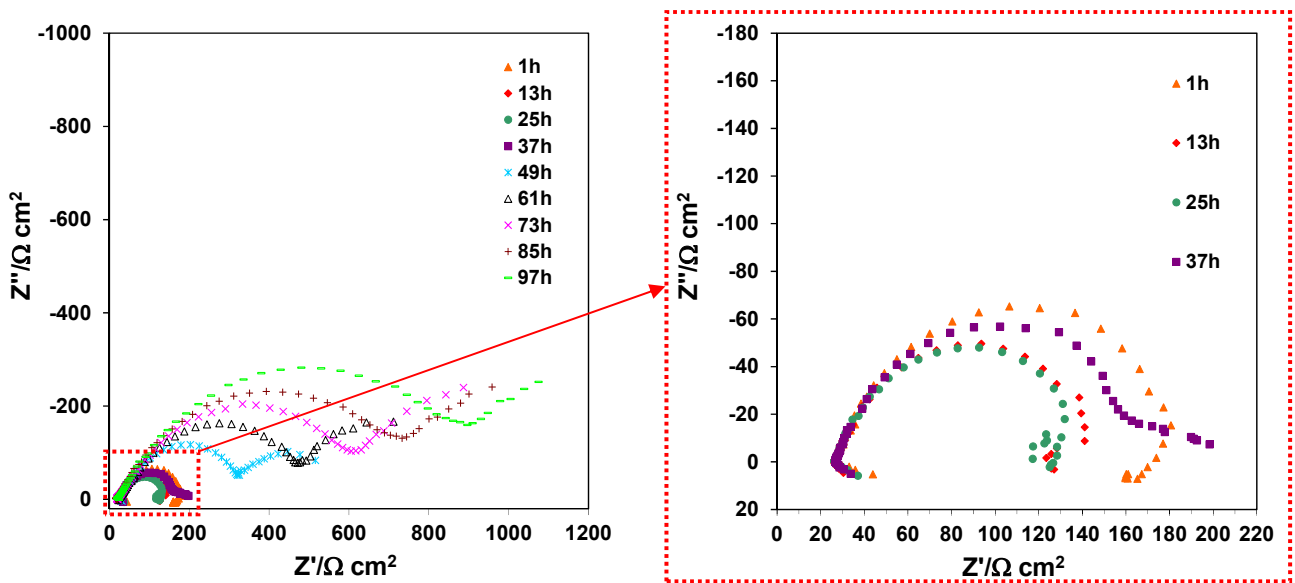
Figure 2: Nyquist plots for X65 carbon steel at different scale formation times in the 0.1 M NaCl and 1 mM $FeCl_2$ solution saturated with CO_2 at 80 ºC.

A capacitive semicircle can be observed at high frequencies in all the Nyquist plots. At 1, 13 and 25h, the Nyquist plots exhibit an inductive loop in the low frequency region, which disappears after 37h of scale formation. The inductive loops in the low frequency range at scale formation times shorter than 37 hours is consistent with the steel dissolution at this stage following a consecutive mechanism with an intermediate product, probably $(FeOH)_{ads}$, adsorbed on the electrode surface according to the following reactions:[12-15]

$$Fe + H_2O \longleftrightarrow (FeOH)_{ads} + H^+ + e^- \qquad (1)$$

$$(FeOH)_{ads} \rightarrow FeOH^+ + e^- \qquad (2)$$

$$FeOH^+ + H^+ \longleftrightarrow Fe^{2+} + H_2O \qquad (3)$$

The previous results indicate that the corrosion scale formed initially on the X65 sample surface was loose and non-protective. After 37 hours, the $FeCO_3$ scale formed on the electrode surface became

more adherent. As the formation of $FeCO_3$ proceeded, it provided increased protection to the steel substrate. Consequently, the inductive loop disappeared and the size of the capacitive semicircle at high frequencies increased with increasing scale formation time. Therefore, this semicircle can be related to the growth of the protective scale on the electrode surface. Besides, a new time constant can be generated in the intermediate-low frequency range (37-97 h). The appearance of this new time constant may be associated with a bi-layer structure of the surface scale. In a recent study, Li et al. [16] suggested the formation of a scale with a bi-layer structure, the outer layer being more porous and the inner layer being more compact. In that work, the authors also considered the possibility of minor iron oxide phases existing in the inner part of the surface scale, modifying the electrical conductivity of the $FeCO_3$ corrosion product layer, i.e., making it an electronic conductor. In a different study, Rosas-Camacho et al. [17] considered that the inner layer of the scale was formed by defective magnetite (Fe_3O_4), while the outer layer was precipitated $FeCO_3$. In any case, observing the EIS spectra in Figure 2 after 37 hours of immersion, it is apparent that at least two different layers are part of the surface scale. Additionally, observing the EIS spectra obtained at immersion times longer than 37 hours (Figure 3), a small time constant can be discerned in the region of very high frequencies (labelled as A in Figure 3), followed by a 45º straight line and a capacitive semicircle at intermediate frequencies (labelled as B in Figure 3) and another capacitive semicircle at low frequencies (labelled as C in Figure 3). The 45º straight line and the subsequent capacitive semicircle (B) are features typical of a Warburg impedance with transmissive boundary condition.
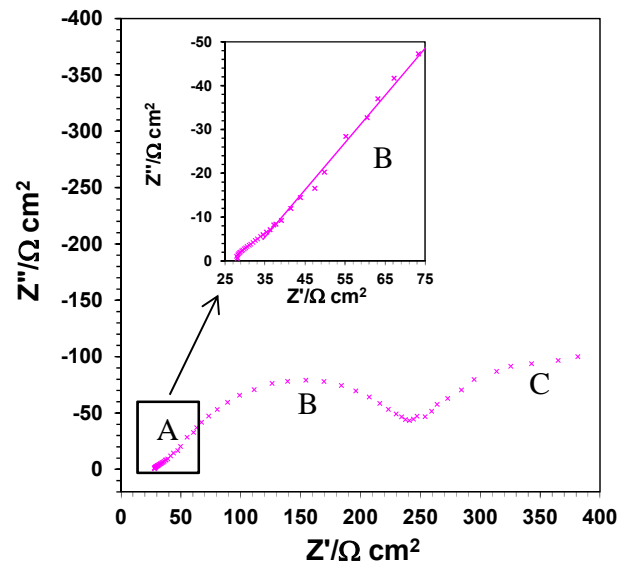
Figure 3: Nyquist plots of X65 steel after 73 hours of scale formation. A small capacitive semicircle can be observed at high frequencies (A), followed by a straight line with a 45º slope and a second capacitive semicircle at intermediate frequencies (B), and a third capacitive semicircle at low frequencies (C).

On the basis of the previous explanations, it is possible to propose equivalent circuits capable of explaining the experimental EIS results obtained at the different immersion times. Figure 4 presents the two equivalent circuits used to fit the experimental EIS data representing the evolution of the substrate/electrolyte interface during scale.
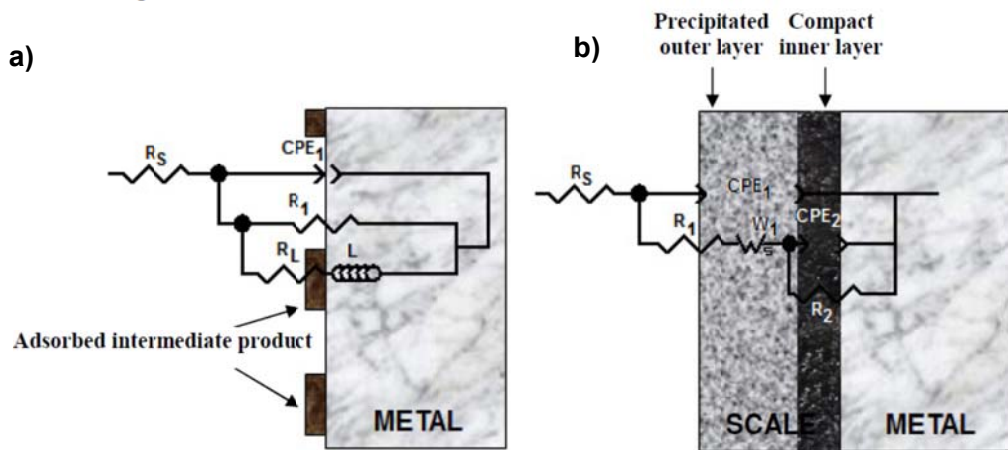
Figure 4: Schematic representation of the evolution of the substrate/electrolyte interface during the scale formation process (a) at short formation times (< 37 h) and (b) at long formation times (> 37 h).

In the equivalent circuits shown, R_S is electrolyte resistance, CPE_1 is related to the capacitance of the substrate/electrolyte interface, R_1 is the resistance at the substrate/electrolyte interface, W_S (with transmissive boundary condition) is the Warburg impedance associated with the diffusion of ions through the precipitated outer $FeCO_3$ layer, and the time constant R_2-CPE_2 is related to the compact inner layer of the scale. Constant phase elements are used in place of capacitors to compensate for non-homogeneity in the system.[18] The Warburg element may be substituted by a parallel R-CPE time constant without affecting the magnitude of the least-squares fit. However, from a physical point of view, it seemed more appropriate to include the Warburg impedance in the equivalent circuit, since this allowed the mass transfer through the corrosion scale to be taken into account.

Table 3 presents the main circuit parameters calculated for different scale formation times. The conversion of CPE into pure capacitance, C, has been performed by means of the following equation:[19;20]

$$C = \frac{(Q \cdot R)^{\frac{1}{n}}}{R} \tag{4}$$

where Q is the impedance of the CPE and R corresponds to R_2 when determining capacitance values of the second time constant. On the other hand, to determine C_1 from CPE_1, R has been calculated on the basis that when a porous layer is present the electrolyte can penetrate through the layer and the distribution of time constants occurs laterally due to this porosity:

$$\frac{1}{R} = \frac{1}{R_S} + \frac{1}{R_1} \tag{5}$$

Values of x^2 are of the order of 10^{-3} or even lower (Table 3), indicating that the model fitting is good from a mathematical point of view. It can be observed that the charge transfer resistance at the substrate/electrolyte interface, R_1, decreased with scale formation time up to 37 hours. After 37 hours of immersion, R_1 values were of the same order of magnitude as R_S values and did not show a clear tendency with formation time, remaining approximately stable during the $FeCO_3$ growth. Thus, at immersion times longer than 37 hours R_1 can be assumed to be equal to the resistance of the electrolyte inside the pores near the scale/electrolyte interface.

Table 3. EIS circuit parameters of X65 steel at different scale formation times in the 0.1 M NaCl and 1 mM $FeCl_2$ solution saturated with CO_2 at 80 ºC.

Time (h)	R_S (Ω cm^2)	R_1 (Ω cm^2)	C_1 (μF cm^{-2})	n_1	R_w (Ω cm^2)	R_2 (Ω cm^2)	C_2 (F cm^{-2})	n_2	R_p (Ω cm^2)	x^2 (x10^{-3})
1	20	180	281	0.80					200	2.2
13	23	71	574	0.78					94	1.1
25	24	66	599	0.83					90	2.5
37	20	25	131	0.70	80	100	0.095	0.95	225	2.0
49	23	18	92	0.70	144	211	0.068	0.94	396	1.0
61	22	10	9	0.62	231	377	0.043	1.00	640	0.5
73	19	21	12	0.64	452	563	0.026	0.90	1055	0.5
85	18	26	10	0.62	503	613	0.024	0.94	1161	1.0
97	18	57	14	0.63	585	678	0.018	0.89	1338	0.6

Considering C_1, its value increased with formation time up to 37 hours indicating, along with the R_1 values, an activation of the Fe dissolution process to form Fe^{2+} cations. At longer formation times (37 hours and longer), C_1 started decreasing until it reached very low values at 97 hours, typical of protective surface layers. This fact indicates that during the scale formation process, C_1 can be associated with the low conductive precipitated outer $FeCO_3$ layer. The exponent of CPE_1 (n_1) exhibited approximately constant values up to 37 hours and then it decreased. This decrease may imply an increase in the heterogeneity of the interface and can be explained by the formation of a rough and porous $FeCO_3$ layer on the electrode surface.[12] On the other hand, n_1 values close to 0.5 may also indicate the appearance of a mass transfer process in the system, which justifies the inclusion of a Warburg element in the equivalent circuit shown in Figure 4 b).

After 37 hours of scale formation, the Warburg resistance R_W increased with increasing formation time, since the precipitated scale presented a diffusion barrier for the species involved in the corrosion process and prevented the underlying metal from further dissolution.

The resistance of the inner layer, R_2, also increased with immersion time. R_2 values increase with increase in the immersion time, reaching high values after 97 hours. The capacitance of the inner layer, C_2, was very high, with values of the order of 18 x 10^{-2} F/cm^2 at the end of the scale formation process. These results indicate that the inner layer has limited insulating properties. According to Li's study.[16], the presence of compositional metal phases or iron oxide phases may significantly change the electrical conductivity of the $FeCO_3$ corrosion product layer. The values of n_2 close to unity suggest the formation of a compact inner layer.

Therefore, according to the EIS results, a possible mechanism of scale formation can be established; after 97 hours of scale formation, the outer precipitated layer of $FeCO_3$ exhibited low electrical conductivity and acted as a diffusion barrier, while the role of the compact inner layer was to cover the steel surface, thereby retarding anodic dissolution of iron. However, the presence of minor phases may cause this inner layer to behave as an electronic conductor.[16] This fact indicates that the protection mechanism of the scale formed on the steel surface is controlled by both the diffusion of species through the scale and a blocking effect at the steel/scale interface.

Figure 5 shows the variation of the corrosion rate (CR) with scale formation time calculated using the polarisation resistance (R_P) obtained by means of the EIS and the LPR, respectively. The variation of the OCP with time is also represented in Figure 5.
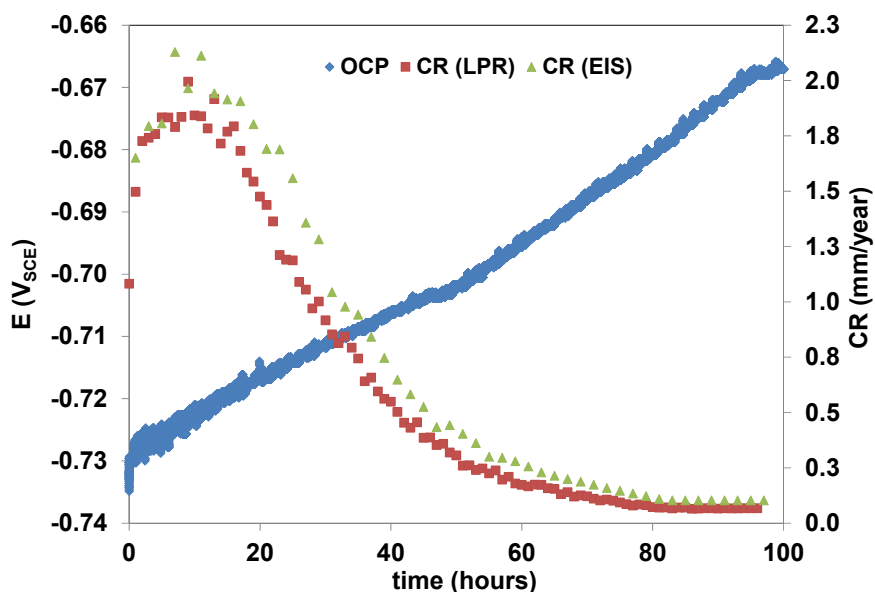
Figure 5: OCP and CR variations (calculated using EIS and LPR measurements) with respect to scale formation time.

It can be observed from Figure 5 that the OCP shifted towards less negative values with increasing scale formation time. The difference between the OCP of the $FeCO_3$ covered surface at the end of the scale formation experiment and the OCP of the bare steel surface at the beginning of the test is ~ 60 mV_{SCE}. This result implies that, with the scale being conductive, when galvanically coupled, the scale covered surface would behave as the cathode of the pair, whereas the bare surface would act as the anode and would corrode faster than uncoupled. This statement can be checked by using a ZRA technique to measure the galvanic pair between both samples.

The value of CR remained approximately constant during the first 5-25 hours of formation, and then started to decrease until reaching values around 0.1 mm/y. These results indicate that when initially exposed to the CO_2 saturated solution, the steel surface started corroding rapidly at first and after 25 hours the R_P increased and the CR decreased, denoting the formation of a protective scale on the steel surface, preventing it from undergoing further dissolution.

The scales formed were characterised by means of X-ray diffraction (XRD) analysis. Figure 6 a) shows an XRD spectrum obtained with a grazing incidence angle of 3 degrees. In this spectrum $FeCO_3$ can be detected in the outer scale. Figure 6 b) presents a confocal image of the scale formed during this stage where the crystals of siderite can be observed.
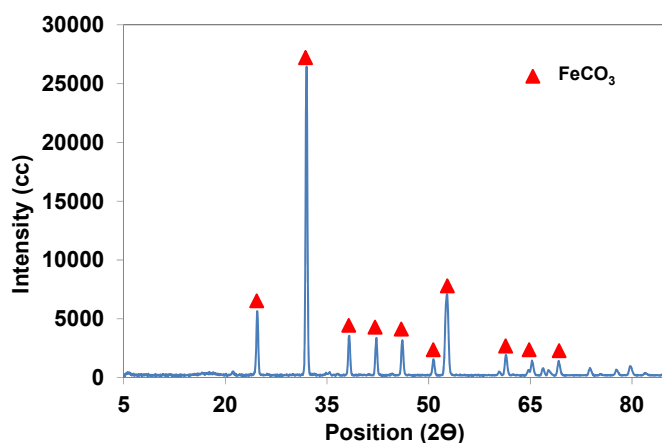
| a) XRD spectrum (3 degrees incidence) | b) confocal image of the scale formed on X-65 |

Figure 6: a) XRD spectrum of the scaled sample obtained with a grazing incidence angle of 3 degrees. b) Confocal image of the scaled sample after 97 hours of immersion in the 0.1 M NaCl and 1 mM $FeCl_2$ solution saturated with CO_2 at 80 ºC.

Galvanic Coupling Tests

Galvanic coupling between two X65 carbon steel electrodes, one with its surface covered by a stable protective scale and the other with a bare surface, was studied using zero resistance ammetery (ZRA). Different tests were performed, modifying the area ratio between both electrodes ($A_R = A_{scaled}/A_{bare}$). Figure 7 shows the galvanic potential (E_G) and galvanic current density (i_G) recorded for 24 hours of galvanic coupling with different area ratios. Galvanic current densities were calculated based on the anode surface area. The positive sign of galvanic current density indicated that, in all the cases, the bare surface electrode was the anode of the pair.

It can be observed from Figure 7 a), for the case of $A_R = 1$, that i_G reached values higher than 15 $\mu A/cm^2$ during the first hour of galvanic coupling, but then decreased continuously until the end of the 12th hour finally reaching an approximately constant value of 3.6 $\mu A/cm^2$. This behaviour of i_G is typical of systems under the formation of a protective surface layer. Therefore, for this area ratio, it is suggested that after 24 hours the galvanic effect was not important between the scaled and the bare electrodes. This result is due to the gradual formation of corrosion product on the anode surface, which may partially and temporally hinder the release of iron. The evolution of E_G with time confirms that, since at the beginning of the test E_G was close to the OCP value of a bare electrode, however after 24 hour of galvanic coupling the E_G value tended to be closer to the OCP of a scaled electrode, indicating that the driving force of the galvanic pair decreased (the OCP of both cathode and anode tended to equalise) and, consequently, i_G values decrease.

An increase in the area ratio to $A_R = 50$ and $A_R = 100$ resulted in higher galvanic current densities, Figures 7 b) and c) respectively. In both cases, the final values of i_G and E_G were very similar, (between 120 and 130 $\mu A/cm^2$). At the beginning of the test performed with $A_R = 50$ and during the whole test with $A_R = 100$, the i_G signal is different from that observed in the case $A_R = 1$, showing many peaks with high amplitudes. The fluctuations in the i_G signal were also accompanied by fluctuations in the galvanic potential signal but with significantly lower amplitudes. This behaviour is related to localised events taking place on the anode surface.[21]

Finally, an additional increase in the area ratio to $A_R = 200$ caused a further increase in galvanic current densities, as shown in Figure 7 d). In this case, the ample oscillations in the i_G signal could also be

observed. As it has been commented previously, these features observed in the i_G vs. time graph are typical of systems undergoing localised events.
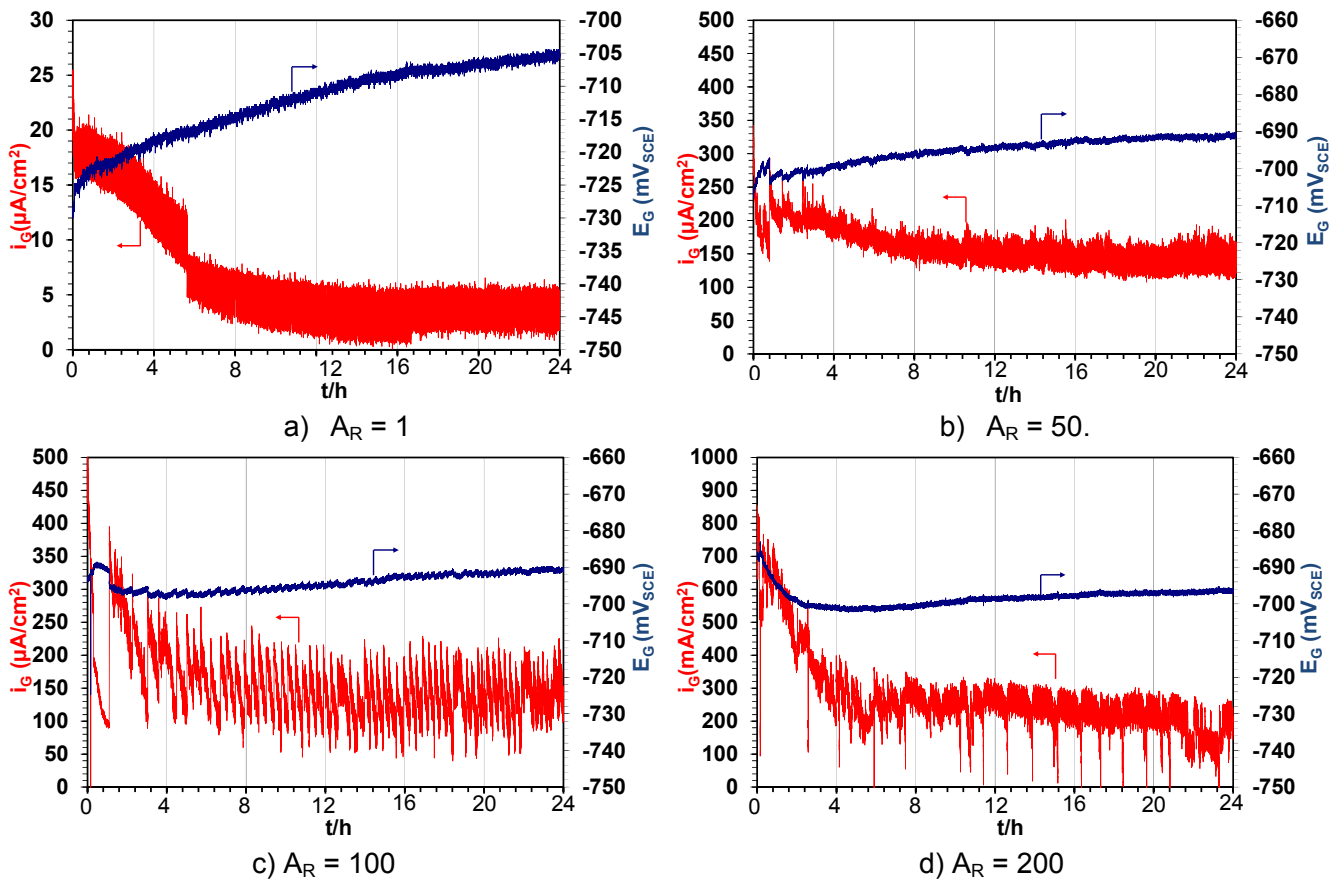
Figure 7: Evolution of the galvanic current density (i_G) and the galvanic potential (E_G) during the galvanic coupling, a) area ratio $A_R = 1$, b) area ratio $A_R = 50$, c) area ratio $A_R = 100$, d) area ratio $A_R = 200$.

The results obtained from the ZRA tests indicate that there is a galvanic effect when a scaled sample is coupled with a bare sample, the last one being the anode of the pair in all the cases. Thus, the scale formed during the first step may present certain conductivity, which allows to establish the galvanic pair between both samples.

A comparison of i_G with different values of A_R is presented in Table 4. It can be observed that with $A_R = 1$, a galvanic effect on the anode of the pair barely existed. An increase of A_R resulted in a very significant increase in i_G, especially in the case $A_R = 200$. Therefore, it can be concluded that the higher the area ratio between the scaled and the bare samples, the more severe the galvanic effect on the anode of the pair (bare sample). This behaviour is coincident with the model developed by Han and co-workers.[22] In general, under static conditions, galvanic corrosion often depends on the rate of diffusion of species to the cathode and the weight loss is independent of the size of the anode and proportional to the area of the cathode metal surface. For a constant area of cathodic metal, the weight loss of the anodic metal is constant. If the area of anodic metal decreases the intensity of corrosion increases as the electric current which flows, concentrates on a smaller area. Therefore, the loss of material is faster and localised leading to the growth of pits.

Furthermore, a reduction in the anode area led to higher fluctuations in the i_G signal. These fluctuations can be due to the formation of corrosion product on the surface of the bare sample, which temporally

hinders the corrosion process. When the corrosion product spread out in the solution, the corrosion process begins again with the current increasing quickly.

Table 4: Influence of the area ratio (A_R = A_{scaled}/A_{bare}) on the galvanic current density (i_G) obtained after 24 hours of galvanic coupling between a scaled surface (cathode) and a bare surface (anode).

A_R = A_{scaled}/A_{bare}	1	50	100	200
i_G ($\mu A/cm^2$)	3.8 ± 0.12	119.2 ± 21	133.1 ± 9.	263.0 ± 43

Figure 8 presents a comparison of the corrosion rate obtained with the galvanic coupled samples (A_R = 50, 100 and 200) and the one obtained with the uncoupled sample. It can be observed that the corrosion rate increases as a consequence of the galvanic coupling, this effect being quite remarkable in the case of the A_R = 200.
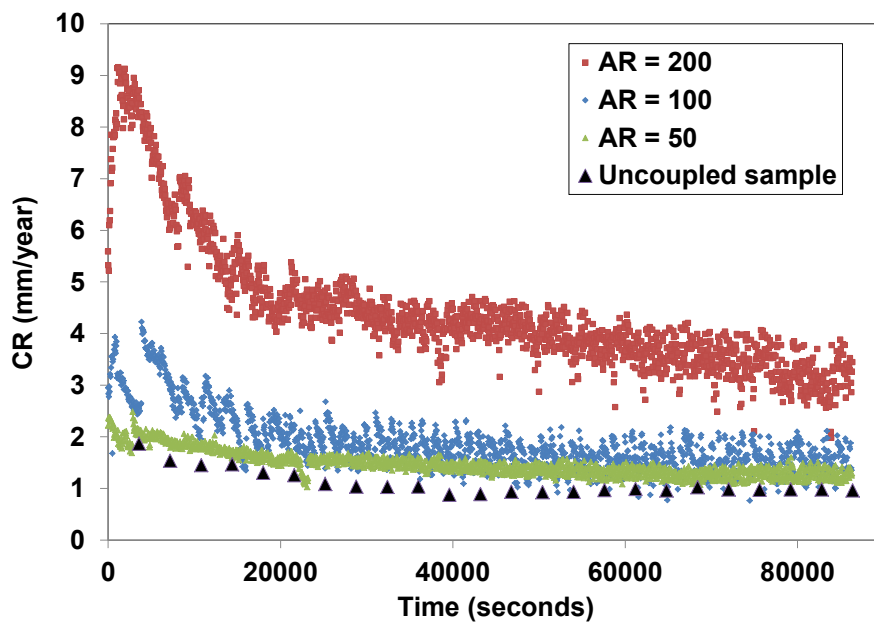
Figure 8: Evolution of the corrosion rate with time of the uncoupled X-65 and of the X-65 coupled with different ratios (A_R = 50, 100 and 200) in the brine solution at 60 ºC saturated with CO_2.

CONCLUSIONS

Conclusions can be summarised as follows:

1. At 80 ºC, 1mM $FeCl_2$, pH 6.8 and CO_2 partial pressure of 0.53 bar a protective scale was formed on the surface of the X-65 after 97 hours, the corrosion rate being around 0.1 mm/year in the end of the tests.
2. The protective scale formed on the surface was probably a bilayer structure which decreases the diffusion of species throughout and has a blocking effect at the steel/scale interface.
3. There was galvanic coupling between the bare metal and a scaled surface, with the bare metal becoming the anode. This indicates that the formed scale presents certain conductivity, which allow establish a galvanic pair.

4. The magnitude of the galvanic pair was found to be dependent on the anode:cathode ratio. Therefore, when the ratio is more unfavourable to the anode, the galvanic current density is greater and the pits can grow faster and deeper.

ACKNOWLEDGEMENTS

REFERENCES

1. M. Ueda, H. Takabe, "Effect of environmental factor and microstructure on morphology of corrosion products in CO_2 environments" NACE CORROSION/1999. paper no 13 (Houston, TX: NACE International, 1999)

2. A. Dugstad, "Mechanism of protective film formation during CO_2 corrosion of carbon steel," CORROSION/1998 paper no 31 (Houston, TX: NACE International, 1998) p 11.

3. J.L. Crolet, N. Thevenot, S. Nešic, " Role of Conductive Corrosion Product in the Protectiveness of Corrosion Layers " *Corrosion* 54, 3, (1998) 194-203.

4. G. Schmitt, T.Gudde, E. Strobel-Effertz, "Fracture Mechanical Properties of CO_2 Corrosion Product Scales and Their Relation to Localized Corrosion," CORROSION/1996, paper no.9, ((Houston, TX: NACE, 1996) p 21.

5. G. Schmitt, M. Mueller, "Critical Wall Shear Stresses in CO_2 Corrosion of Carbon Steel," CORROSION/1999, paper no.44, ((Houston, TX: NACE International, 1999) p 14.

6. G. Schmitt, S. Feinen, "Effect of Anions and Cations on The Pit Initiation in CO_2 Corrosion of Iron and Steel," CORROSION/2000, paper no.1, (Houston, TX: NACE International, 2000) p 15.

7. R. Nyborg, "Initiation and Growth of Mesa Corrosion Attack During CO_2 Corrosion of Carbon Steel," CORROSION/1998, paper no.48, (Houston, TX: NACE International, 1998) p 13.

8. K.S. George, S. Nešic. Investigation of Carbon Dioxide Corrosion of Mild Steel in the Presence of Acetic Acid, Part I - Basic Mechanisms. *Corrosion* 63, 2, (2007) 178-188.

9. J. Han, Y. Yang, B. Brown, S. Nešic. "Electrochemical Investigation of Localized CO_2 Corrosion on Mild Steel". CORROSION/2007 paper no 07323 (Houston, TX: NACE International, 2007) p 12.

10. J. Han, B.N. Brown, S. Nešic. "Investigation of the Galvanic Mechanism for Localized Carbon Dioxide Corrosion Propagation Using the Artificial Pit Technique" *Corrosion* 66, 9 (2010) . 095003-1 - 095003-12.

11. G.A. Zhang, Y.F. Cheng. "Localized corrosion of carbon steel in a CO_2-saturated oilfield formation water". *Electrochimica Acta* 56, 3, (2011) 1676-1685.

12. F. Farelas, M. Galicia, B. Brown, S. Nešic, H. Castaneda. " Evolution of dissolution processes at the interface of carbon steel corroding in a CO_2 environment studied by EIS" *Corrosion Science* 52, 2, (2010) 509-517.

13. J.B. Sun, G.A. Zhang, W. Liu, M.X. Lu, "The formation mechanism of corrosion scale and electrochemical characteristic of low alloy steel in carbon dioxide-saturated solution" *Corrosion Science* 57, 4, (2012) 131-138.

14. S. Guo, L. Xu, L. Zhang, W. Chang, M. Lu. " Corrosion of alloy steels containing 2% chromium in CO_2 environments" *Corrosion Science* 63, 10, (2012) 246-258.

15. J. O. M. Bockris, D. Drazic, and A. R. Despic, "The electrode kinetics of the deposition and dissolution of iron" *Electrochimica Acta*, 4, 2-4, (1961) 325-361.

16. W. Li, B. Brown, D. Young, S. Nešic. "Investigation of Pseudo-Passivation of Mild Steel in CO2 Corrosion" *Corrosion* 70, 3, (2014) 294-302.

17. O. Rosas-Camacho, M. Urquidi-Macdonald, D.D. Macdonald, " Deterministic Modeling of the Corrosion of Low-Carbon Steel by Dissolved Carbon Dioxide and the Effect of Acetic Acid. I-Effect of Carbon Dioxide". *ECS Transactions* 19, 29, (2009) 143-165.

18. Wu, Cui, Zhao, Yan, Zhu, Yang. "EIS study of the surface film on the surface of carbon steel from supercritical carbon dioxide corrosion" *Applied surface science* 228, 1-4, (2004) 17-25.

19. G.J. Brug, A.L.G. van den Eeden, M. Sluyters-Rehbach, J. H. Sluyters. " The analysis of electrode impedances complicated by the presence of a constant phase element" *Journal of Electroanalytical Chemistry* 176 (1984) 275-295.

20. B. Hirschorn, M.E. Orazem, B. Tribollet, V. Vivier, I. Frateur, M. Musiani. " Determination of effective capacitance and film thickness from constant-phase-element parameters" *Electrochimica Acta* 55 (2010) 6218-6227.

21. A. Legat, V. Dolecek. "Corrosion Monitoring System Based on Measurement and Analysis of Electrochemical Noise" *Corrosion* 51, 4, (1995) 295-300.

22. J. Han, S. Nešic. B. N. Brown. "Galvanic model for localised corrosion" CORROSION/2009 paper no 2687 (Houston, TX: NACE International, 2009) p 15.